Estuarine, Coastal and Shelf Science 130 (2013) 42–53

Contents lists available at SciVerse ScienceDirect

Estuarine, Coastal and Shelf Science

journal homepage: www.elsevier.com/locate/ecss

Vertical accumulation of potential toxic elements in a semiarid system that is influenced by an abandoned gold mine

Martha A. Sánchez-Martínez, Ana J. Marmolejo-Rodríguez*, Víctor R. Magallanes-Ordóñez, Alberto Sánchez-González

Centro Interdisciplinario de Ciencias Marinas del Instituto Politécnico Nacional, Av. IPN s/n, Col. Playa Palo de Sta. Rita, 23096 La Paz, Baja California Sur, Mexico

ARTICLE INFO

Article history:
Received 11 September 2012
Accepted 19 March 2013
Available online 16 April 2013

Keywords:
sediment
trace elements
mine zone
potential toxic elements

ABSTRACT

The mining zone at El Triunfo, Baja California Sur, Mexico, was exploited for gold extraction for 200 years. This area includes more than 100 abandoned mining sites. These sites contain mine tailings that are highly contaminated with potential toxic elements (PTE), such as As, Cd, Pb, Sb, Zn, and other associated elements. Over time, these wastes have contaminated the sediments in the adjacent fluvial systems. Our aim was to assess the vertical PTE variations in the abandoned mining zone and in the discharge of the main arroyo into a small lagoon at the Pacific Ocean. Sediments were collected from the two following locations in the mining zone near the arroyo basin tailings: 1) an old alluvial terrace (Overbank) and a test pit (TP) and 2) two sediment cores locations at the arroyo discharge into a hypersaline small lagoon. Samples were analyzed by ICP-MS, ICP-OES, and INAA and the methods were validated. The overbank was the most contaminated and had As, Cd, Pb, Sb, and Zn concentrations of 8690, 226, 84,700, 17,400, and 42,600 mg kg^{-1}, respectively, which decreased with depth. In addition, the TP contained elevated As, Cd, Pb, Sb, and Zn concentrations of 694, 18.8, 5001, 39.2, and 4170 mg kg^{-1}, respectively. The sediment cores were less contaminated. However, the As, Cd, Pb, Sb, and Zn concentrations were greater than the concentrations that are generally found in the Earth's crust. The normalized enrichment factors (NEFs), which were calculated from the background concentrations of these elements in the system, showed that extremely severe As, Cd, Pb, Sb, and Zn (NEF $>$ 50) enrichment occurred at the overbank. The TP was severe to very severely enriched with As, Cd, Pb, Sb, and Zn (NEF = 10–50). The sediment cores had a severe enrichment of As, Pb, and Zn (NEF = 10–25). Their vertical profiles showed that anthropogenic influences occurred in the historic sediment deposition at the overbank and TP and in the sediment cores. In addition, the As, Pb, and Zn concentrations in the sediment cores were related to the deposition of fine sediments and organic carbon.

1. Introduction

Mine tailings and residual waters release large quantities of trace elements into the environment (Nriagu and Pacyna, 1988; Salomons, 1995). These wastes are rich in potential toxic elements (PTE) and are abandoned without protecting the adjacent biota. These PTE are widely distributed and become concentrated in fluvial sediments, agricultural and natural soils, vegetables, and surface and subsurface waters. The most commonly studied PTE include As, Cd, Pb, and Zn (Audry et al., 2004; Bodénan et al., 2004; Borrego et al., 2004; Bhattacharya et al., 2006; Krysiak and Karczewska, 2007; Lim et al., 2008; Taylor and Hudson-Edwards, 2008; Da Pelo et al., 2009; Meza-Figueroa et al., 2009; Navarro-Flores and Doménech-Rubio, 2010; Perner et al., 2010; Rashed, 2010; Romero et al., 2010). However, few studies have focused on semiarid systems where contamination is exacerbated by wind transport of fine mine tailing particles during the rainy season (Taylor and Hudson-Edwards, 2008; Meza-Figueroa et al., 2009; Navarro-Flores and Doménech-Rubio, 2010). The historical evolution of mining activities and natural extreme events (e.g., tropical storms and hurricanes) are known (Price et al., 2005; Kovács et al., 2006). Thus, geochemical studies regarding the vertical distribution of PTE were conducted to characterize the temporal variation of the PTE. In addition, we aimed to determine if the contaminated tailings that were produced by historical mining activities were deposited in fluvial and coastal sediments and if PTE accumulated at or were leached from the final disposal sites. Thus, the objective of

* Corresponding author. Permanent address: Oceanology Department, Centro Interdisciplinario de Ciencias Marinas del Instituto Politécnico Nacional (CICIMAR-IPN), Av. IPN s/n, Col. Playa Palo de Sta. Rita, 23096 La Paz, BCS, Mexico.
E-mail address: amarmole@ipn.mx (A.J. Marmolejo-Rodríguez).

0272-7714/$ – see front matter © 2013 Published by Elsevier Ltd.
http://dx.doi.org/10.1016/j.ecss.2013.03.017

this research is to characterize the vertical distribution of As, Cd, Pb, Sb, and Zn in the El Triunfo mining zone, B.C.S., and in the arroyo discharge that leads to the Pacific Ocean. From these results, the influence of the mine wastes on the vertical accumulation and enrichment of PTE at the source and destination of the main arroyo will be determined.

2. Materials and methods

2.1. Study area

The mining zone of El Triunfo is in the State of Baja California Sur, Mexico, which is 45-km south of La Paz, B.C.S. (Fig. 1). The climate is dry and semiarid with sporadic rain in December and more during the summer. This summer rainy season results from hurricanes and tropical storms (Troyo-Diéguez et al., 1990). Furthermore, this zone is located in the Cabo San Lucas block and is dominated by igneous intrusive rocks, such as gabbro, granodiorite, and granite. In addition, metamorphic rocks, such as the garnet schists and gneisses are present in this fluvial system (COREMI, 1999). The ore that is mined occurs in epithermal veins that contain sulfur minerals and associated Au and Ag. These minerals include pyrite, arsenopyrite, sphalerite, and galena (Carrillo, 1996). This mine was exploited for Au and Ag from the middle of the XVIII century. There are hundreds of abandoned mining sites, of which approximately 30 contain tailing piles (Carrillo, 1996). The mine zone is connected to the Pacific Ocean

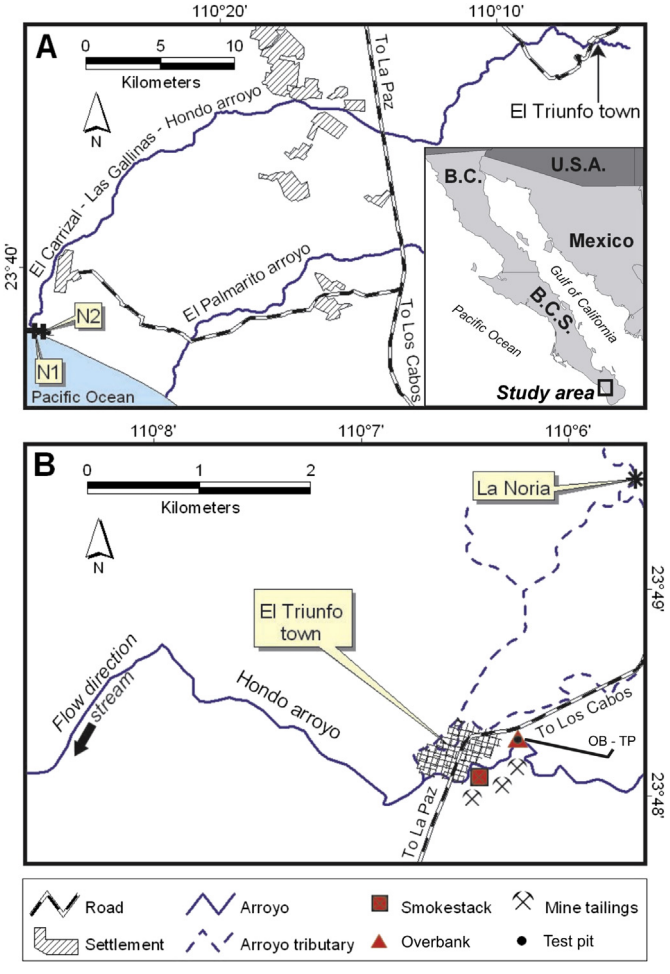

Fig. 1. Map of the study area. A) shows the town of El Triunfo, La Noria, and the location of the overbank and the test pit. B) shows the arroyo discharge. Cores 1 and 2 are located at the evaporitic basin that is adjacent to the Pacific Ocean.

in the southwest by the Hondo – Las Gallinas – El Carrizal (H–G–C) arroyo. This arroyo discharges into an evaporitic basin that extends along the cost, which accumulates water during heavy rains. Previous regional studies have measured the PTE concentrations in mining wastes, soils, and vegetables (Carrillo, 1996; Acosta et al., 2000; Volke-Sepúlveda et al., 2003; Naranjo, 2004). In addition, geochemical studies were conducted regarding the migration of the PTE throughout the H–G–C arroyo, which discharges at the Pacific Ocean (Romero-Guadarrama, 2011; Marmolejo-Rodríguez et al., 2011).

2.2. Sampling considerations

Sediments were sampled at the three following sites in the same hydrographical basin: 1) near the mine zone; 2) at the evaporitic basin, and 3) from a clean zone called La Noria (with no mining influence) (Fig. 1A and B).

2.2.1. Near the mine zone

Sediments were obtained from an overbank (OB) with a tailing pile. This OB is an old terrace that is covered by mine wastes from an old artisanal mine. This OB is near a mining vent from which gold was extracted and is located (23°48'16.40″N 110° 6'14.60″W; 493 m above sea level – masl) in a meander of the arroyo that is approximately 490-m NE of the main smokestack. Sediments were also obtained from a test pit (TP). The TP was sampled by excavating the arroyo Hondo sediments at approximately 4 m from the OB (23°48'16.27″N 110° 6'14.52″W; 493 masl). These sediments were collected to determine the influence of the OB tailings at a depth of 1-m in the arroyo sediments. The OB and TP sampling sites are in the town of El Triunfo (Fig. 1A).

2.2.2. Evaporitic basin

The evaporitic basin occurs at the discharge of the H-G-C arroyo (the main arroyo from the source to the destination) into the Pacific Ocean (Fig. 1B). However, this arroyo discharges into an evaporitic basin (a small hypersaline lagoon) and not directly into the Pacific Ocean. Here, two sedimentary cores (C1 and C2) were collected. The C1 core was obtained from the central part of the small lagoon (23°37'40.74″N 110°26'41.16″W and 3 masl), which was near the arroyo discharge. At approximately 500 m from the C1, the C2 core was collected from the proximal part of the discharge (23°37'39.00″N 110°26'21.96″W and 6 masl).

2.2.3. La Noria

The background levels were measured in La Noria in the same hydrographical basin. This area is located 2.8 km northeast of El Triunfo (Fig. 1A) (23°49'31.92″N, 110° 5'40.20″ W and 525 masl). La Noria is a small group of rural houses. In addition, this site was less impacted by mining wastes due to its higher altitude (525 masl) than the wastes in the alteration zone (at 493 masl).

2.3. Sampling methods

The polyethylene material was washed with clean techniques that were previously described (Marmolejo-Rodríguez et al., 2011). Sediments were sampled in the three following zones: 1) near the contamination source (OB and TP); 2) two sediment cores near the discharge at the Pacific Ocean, and 3) in La Noria, a clean zone of the hydrographical basin.

2.3.1. Sediment sampled in the mining zone: an overbank and a test pit

Sediments near the mining activities were collected from two different sites. At the OB, arroyo surface sediments were collected

from a 2 m tall vertical trench (Fig. 1A). At the TP, samples were collected approximately 4 m from the overbank. The TP samples were collected to a depth of 90-cm from the arroyo surface. The OB and TP sediments were each collected at 10 cm by beginning with the deeper zones and carefully avoiding sediment mixing. This method was suggested by Taylor and Hudson-Edwards (2008).

2.3.2. Evaporitic basins C1 and C2

In October 2010, two sediment cores (Fig. 1B) were collected with a PVC tube. The sediment cores were 3.6 cm in diameter and 34 cm in length for the C1 core and were 3.6 cm in diameter and 31 cm in length for the C2 core. The sediment cores were cooled, and each centimeter of the core was extruded starting at the uppermost part.

2.3.3. Sediment in La Noria

At 300 m from La Noria, we obtained six different sediment samples from a very small and homogenous alluvial terrace. This measured 40 cm height and the sediment was sampled 5 cm away from the deeper area to the upper part.

2.4. Analytical methods

The samples were dried in a wood-burning oven at 45–50 °C. The total fraction (<2000 μm) of the sediment was pulverized in an agate mortar prior to elemental analyses. Another aliquot of the sediment was used to determine the grain size. The sieve technique was used to quantify the amount of sand and the laser dispersion technique was used to quantify the amounts of silt and clay (Horiba LA-910 in the IIO-UABC laboratory). The total carbon and inorganic carbon concentrations were determined by combustion with a Coulometer (UIC Inc. Mod. CM5015 in the FCM-UABC laboratory). The organic carbon (C_{org}) was estimated as the difference between the total and inorganic carbon. The elemental analyses of As, Cd, Cu, Pb, Sb, Zn, Al, Fe, and Li were conducted by total digestion in HF, $HClO_4$, HNO_3, and HCl. First the samples were digested with HF. Next, the samples were digested in a mixture of HNO_3 and $HClO_4$ while heating at 260 °C. The digested samples were dried and then diluted with HNO_3 and HCl prior to ICP/MS analysis with a Perkin Elmer Sciex ELAN 9000. As and Sb were also analyzed with INAA. All the analyses were realized at Actlabs (Ontario, Canada). The methods were validated with certified materials (PACS-2 and MESS-3). Moreover, one measurement was duplicated for every ten samples analyzed. These duplicate measurements indicated that good reproducibility was obtained. The method validation results are shown in Table 1.

3. Results

3.1. Stratigraphy, grain size, and organic carbon in the microenvironments

The vertical distribution of the grain size and the percentages of C_{org} in the sediments are presented in Figs. 2 and 3.

3.1.1. Sediments in the overbank and the test pit

3.1.1.1. Overbank. The dominant grain size in the OB was sand (66%). The percentages of gravel (27%) and silt and clay (6%) were smaller (Fig. 2a). The grain-size sequence is composed of five lithologic layers. Layer A, with a thickness of 98 cm, is a conglomerate (gravel, very angular) with a sandy matrix. The composition of layer A, suggests the occurrence of an extreme event with a high loading capacity. Layer B has a thickness of 6 cm and is characterized by fine sands. Layer C has a thickness of 30 cm and is composed of fine sands and red silt. Layer D contains 15 cm of fine yellow sand. Finally, layer E is 45 cm thick, is the most recent deposit and is composed of fine red material (tailings) that is mixed with sand and roots. From layers B to E (the last 102 cm), the average gravel content decreases (17%) in comparison with the average sand content (73%). Furthermore, the average silt content increases (11%).

In the first 100 cm (layer A), the C_{org} content is low (<0.1%). In the sandstone layer and in the tailings deposit on top of the old terrace, the C_{org} content significantly increased to a maximum of 1% (Fig. 2a).

3.1.1.2. Test pit. The vertical profile of the TP sediment was obtained 4 m from the OB tailings deposit. The TP depth was 90-cm from the surface sediments of the arroyo. The grain-size was 57% sand and 43% gravel. The silt-clay fraction was only 0.6% (Fig. 2b). The sediment sequence is composed of four layers that are made of sand and conglomerate (pebbles and very angular gravel). Layers A and C resulted from extreme high energy events in which the amount of pebbles and gravel increased relative to that of sand. Layers B and D were deposited during periods of low energy in which the amount of sand increased.

The lowest organic carbon concentration (<0.3%) was observed in these layers due to their lower silt-clay contents. The vertical distribution of C_{org} was not related to the sediment grain-size along the TP (Fig. 2b).

3.1.2. Evaporitic basin

3.1.2.1. Sediment core 1. The C1 sediment core was covered by water. On sampling day, the pH was 8 and the salinity was 130‰. The average grain-size distribution was 17% for fine to very fine sand, 70% for silt, and 13% for clay (Fig. 3a). C1 is composed of 4 layers that are 7.5, 11, 6, and 9.5 cm thick. Layer A contains fine black sediment with a gray lenticular structure. In this layer, silt predominates at an average of 76%. Layer B consists of mud sediments that are predominantly homogenous gray silt (75%). Layer C contains fine yellow sand. In this level, the average silt decreased (62%) and the average fine sand (29%) increased. Layer D is composed of fine black sediments with a gray lenticular structure that is similar to those in layer A. The surface of C1 consists of a 0.5 cm layer of recent organic matter. The mean organic carbon concentration in C1 (Fig. 3a) is 1.7% (0.49–3%). The C_{org} concentration is well-correlated with the silt content, which decreases in the fine sand layers.

3.1.2.2. Sediment core 2. This core was sampled at nearly the end of the evaporitic basin. The pH was 8.94 and the salinity was 140‰ on the day of sampling. The grain-size distribution consisted of 32% fine sand, 56% silt, and 12% clay (Fig. 3b). The three following layers were measured: 1) layer A consisted of 7 cm of mud, 2) layer B was characterized by sand, and 3) layer C consisted of mud. The C_{org} concentrations in these layers were between 0.04% and 3.8%. The C_{org} concentration in layers A and C were >1%, which corresponded to the presence of mud. However, in layer B (the sand layer), the C_{org} content, significantly decreased to <0.2% (Fig. 3b).

3.2. Vertical distributions of Al, As, Cd, Cu, Fe, Sb, Pb, and Zn

3.2.1. Lithogenic elements

The concentrations of Al, Fe, and Li at La Noria are similar to those in the Earth's crust (Table 2). The standard deviation of Al was lower than the standard deviations of the other elements in the sediments. However, their concentrations were different between the mine tailings and ash (Marmolejo-Rodríguez et al., 2011). In the OB, TP, and sediment cores, the mean iron concentrations were higher than in the Earth's crust (Wedepohl, 1995). The highest iron

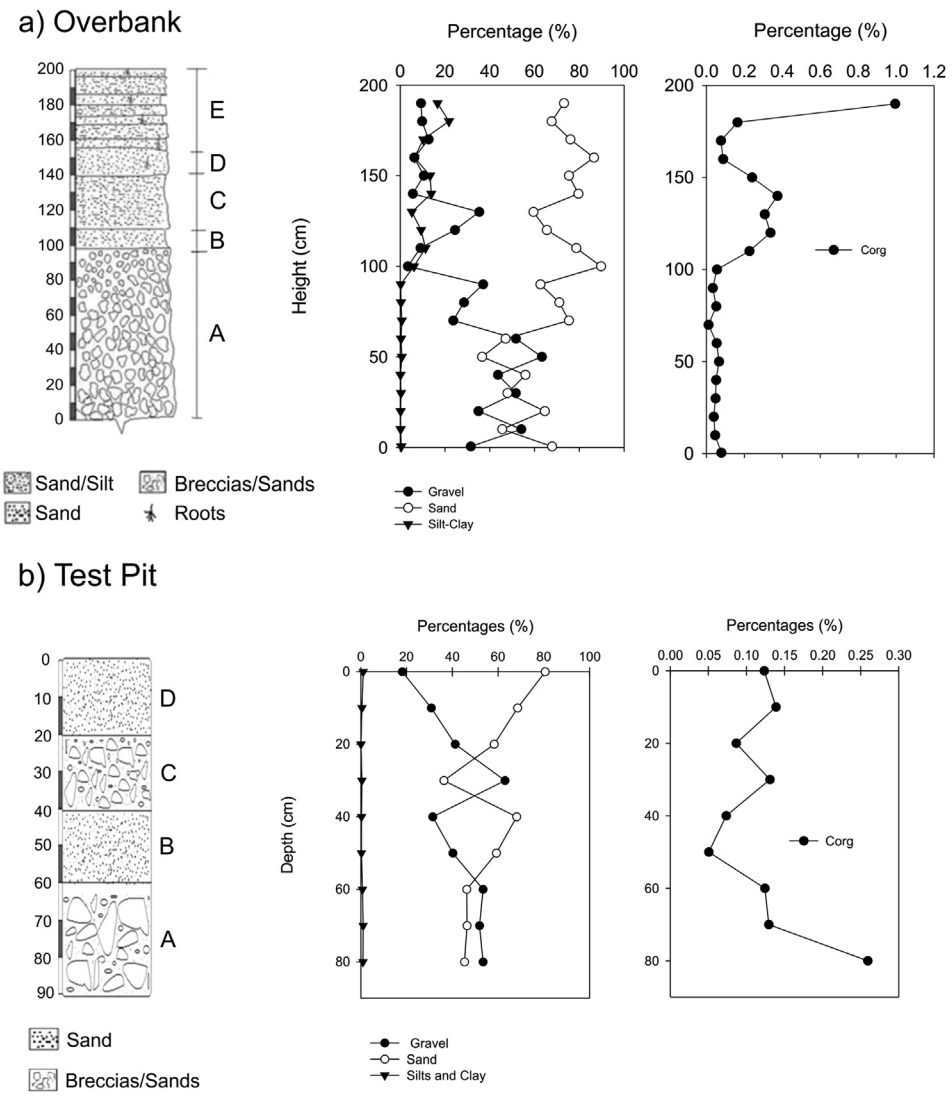

Fig. 2. a) The stratigraphic column of the overbank and the grain-size percentages of gravel, sand, and silt and clay. The percentages of C_{org} are represented by the filled circles. Figure 2. b) Stratigraphic column of the test pit, and the grain-size and C_{org} percentages.

concentrations were present in the tailings, in which oxy-hydroxides were most likely formed. The Li concentration is not homogenous and is highest in C1 and C2. These Li concentrations were greater than in the Earth's crust. Therefore, the Al concentration was used to normalize elemental concentrations in this system.

3.2.2. Trace elements

The concentrations of trace elements in these systems, including their average concentrations in the Earth's crust (Wedepohl, 1995) and the Mexican legislation values (NOM-147-SEMARNAT/SSAI-2004) are presented in Table 2. Mexican legislation has set limits for determining if soil remediation is needed to reduce health risks.

Table 1
Method validation results. Detection limits and concentration obtained and certified by the certified standards (mean ± *s*). The certificate reference materials were PACS-2 and MESS-3 from the National Research Council of Canada.

Element	Detection limits (mg kg^{-1})	PACS-2		MESS-3		%
		Certified	Obtained	Certified	Obtained	Reproducibility
As (mg kg^{-1})	0.1	26.2 ± 1.5	27 ± 1	21 ± 1	22 ± 2	98 ± 12
Cd (mg kg^{-1})	0.1	2.11 ± 0.1	2 ± 0.1	0.24 ± 0.01	0.2 ± 0	98 ± 5
Cu (mg kg^{-1})	0.2	310 ± 12	318 ± 4	33.9 ± 1.6	34.3 ± 1.3	94 ± 7
Pb (mg kg^{-1})	0.5	183 ± 8	186 ± 11	21.1 ± 0.7	25.1 ± 1.0	101 ± 6
Sb (mg kg^{-1})	0.1	11.3 ± 2.6	7.5 ± 1.5	1.02 ± 0.1	1.1 ± 0.1	102 ± 5
Zn (mg kg^{-1})	0.2	364 ± 23	397 ± 12	159 ± 8	156 ± 6	98 ± 8
Li (mg kg^{-1})	0.5	32.2 ± 2	33 ± 0.4	73.6 ± 5	73 ± 1.6	100 ± 3
Al (%)	0.01%	6.62 ± 0.32	6.3 ± 0.14	8.59 ± 0.23	8.2 ± 0.2	99 ± 6
Fe (%)	0.01%	4.1 ± 0.1	3.8 ± 0.05	4.34 ± 0.11	3.9 ± 0.1	98 ± 2

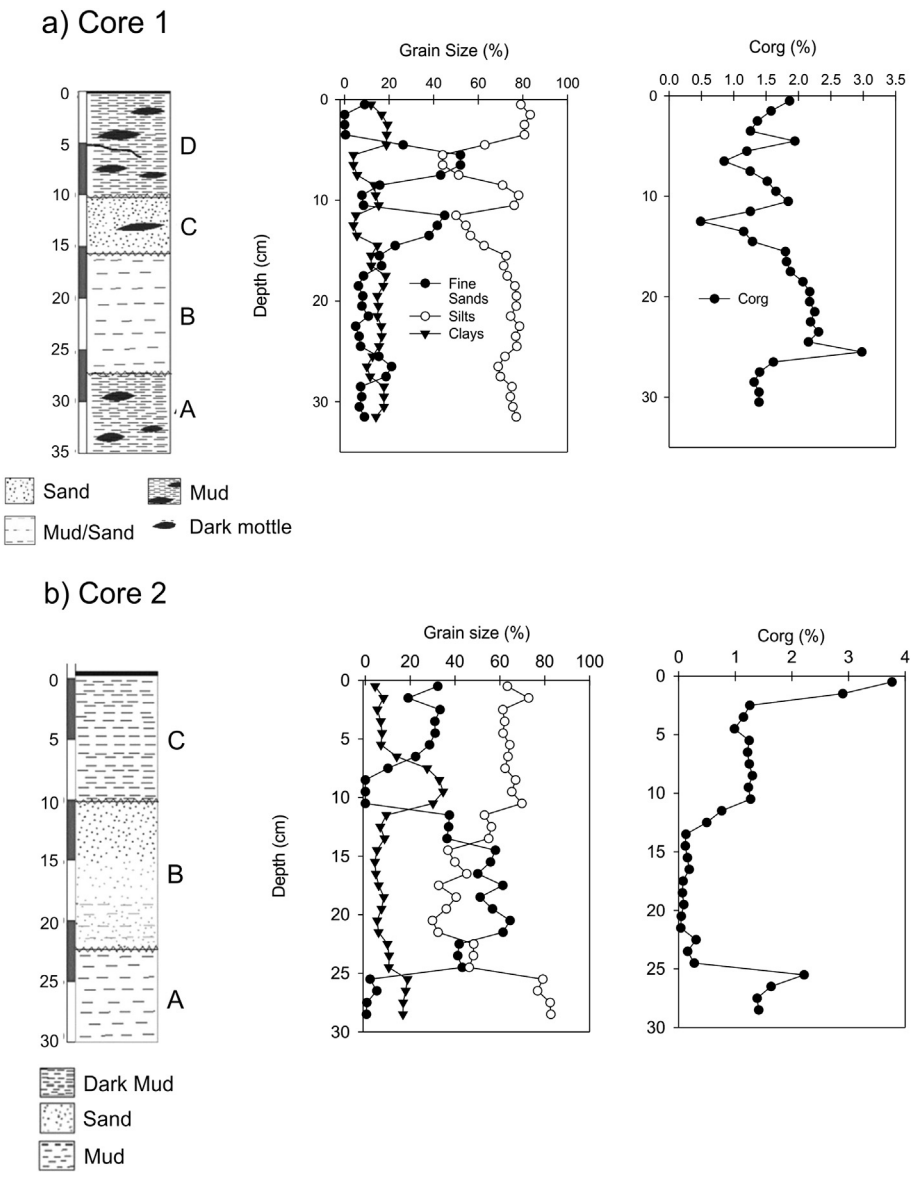

Fig. 3. a) Stratigraphic column of Core 1. The grain-size percentages of fine sand, silt, and clay are shown. The C_{org} is represented by a filled circles. b) Stratigraphic column of Core 2. The grain-size percentages of fine sand, silt, and clay are shown. The C_{org} is shown represented by a filled circles.

The elements studied here are classified as Potential Toxic Elements (PTE).

3.2.2.1. Background values found in La Noria. The samples from La Noria were the least contaminated. These samples had lower PTE concentrations than the OB, TP, and the sediment cores (Table 2). The PTE concentrations at La Noria were similar to the average values that are found in the Earth's crust. Specifically for As, the mean concentrations were only 2.7 times greater than those found by Wedepohl (1995). For Cd and Cu, the concentrations were similar to those in the Earth's crust, but for Pb (0.7) the concentrations were lower. For Sb and Zn, the concentrations were slightly higher than in the Earth's crust. Therefore, in this microenvironment, the PTE are not enriched. Thus, these concentrations were used as regional background values.

3.2.2.2. Overbank on the Hondo arroyo near the alteration zone. The OB is the most contaminated site with maximum As, Cd, Cu, Pb, Sb, and Zn concentrations of 8690, 226, 1510, 84,700, 17,400, and 42,600 mg kg^{-1}, respectively (Table 2). These concentrations are greater than those that are allowed by the Mexican legislation for As, Cd, and Pb and for the Earth's crust.

The vertical profiles of the elemental concentrations were similar between the different elements that were studied here. Overall, these elements were concentrated in the upper layer (100–200 cm) and decreased to the baseline (100 to surface of the arroyo). In the 100–200 cm layer, the elemental concentrations were heterogenous. However, large As, Cd, Cu, Pb, Sb, and Zn concentrations of 264–8690, 32.8–226, 59–420, 1860–84,700, 19–17,400, and 1540–42,600 mg kg^{-1}, respectively, occurred in this layer. The element concentrations were heterogenous, but with lower concentrations toward the surface of the arroyo (Fig. 4).

3.2.2.3. Test pit in the Hondo arroyo near the alteration zone. The TP (approximately 4 m horizontally from the OB samples) had lower elemental concentrations than the OB. Specifically, the TP had maximum As, Cd, Cu, Pb, Sb, and Zn concentrations of 694, 18.8, 157, 5001, 39.2, and 4170 mg kg^{-1}, respectively (Fig. 5). These As and

Table 2
Lithogenic and potential toxic elements (PTE) origin of elements. Mean, standard deviation, minimum and maximum concentrations in the mining zone of El Triunfo: (Overbank and the Test Pit), and in the arroyo mouth of El Carrizal, which discharges at the evaporitic basin adjacent to the Pacific Ocean (Core 1 and Core 2). La Noria as pristine zone of the same fluvial basin, the Earth's crust average (UCC) and the Mexican Legislation (ML) limits are included.

Element	Overbank ($n = 20$)	Test pit ($n = 9$)	Core 1 ($n = 17$)	Core 2 ($n = 15$)	LaNoria ($n = 6$)	UCC	ML
Lithogenics							
Al	5.5 ± 2.6	6.9 ± 1.6	7.8 ± 1.1	7.2 ± 1.4	6.7 ± 0.3	7.74	n.d.
(%)	1.6–8.3	2.8–7.8	5.4–9.5	3.0–.9	6.2–7.1		
Fe	9.0 ± 5.0	5.02 ± 0.9	4.3 ± 0.8	3.2 ± 1.2	3.1 ± 0.3	3.08	n.d.
(%)	3.6–18	3.1–6.3	2.7–5.5	1.4–5.2	1.4–5.2		
Li	10.6 ± 2.6	11.6 ± 2.4	37 ± 6.0	27 ± 13	3.1 ± 0.3	22	n.d.
(mg kg^{-1})	6.7–16.8	8.6–14.8	29–46	11.6–56	2.8–3.5		
PTE							
As	2898 ± 3481	318 ± 151	108 ± 46	46 ± 40	5.48 ± 1.7	2.0	22
(mg kg^{-1})	21–8690	174–694	50.8–186	7.8–112	3.7–8.0		
Cd	67.6 ± 83.2	7.9 ± 4.4	4.0 ± 1.2	1.8 ± 1.6	0.03 ± 0.0	0.102	37
(mg kg^{-1})	0.2–226	5–18.8	1.8–6.3	0.2–4.7	0.0–0.1		
Cu	511 ± 603	59.8 ± 41.5	41 ± 10	25 ± 15	14.6 ± 0.6	14.3	n.d.
(mg kg^{-1})	16.6–1510	27.4–157	58.9–26.2	5.9–55	13.6–15		
Pb	27,079 ± 33,900	1664 ± 1552	402 ± 135	156 ± 144	11.4 ± 1.0	17	400
(mg kg^{-1})	15–84,700	268–5001	172–617	13.6–362	10-13		
Sb	4415 ± 7005	15.5 ± 9.7	16 ± 13	6.6 ± 6.2	0.6 ± 0.48	0.31	n.d.
(mg kg^{-1})	1.2–17,400	9.9–39.2	5.3–55.5	0.5–19.6	0.2–1.5		
Zn	14,248 ± 17,100	1141 ± 1243	278 ± 63	138 ± 88	68.7 ± 5.2	52	n.d.
(mg kg^{-1})	67–42,600	390–4170	186–377	37–281	63–78		

ML = Mexican legislation NOM-147-SEMARNAT/SSAI-2004; UCC = Upper Continental Crust, Wedepohl, 1995.

Pb concentrations were higher than those set by Mexican legislation. The vertical profiles were similar for As, Cd, Cu, and Zn. The maximum concentrations for As, Cd, Cu, Pb, Sb, and Zn were 694, 18.8, 157, 5000, 39.2, and 4170 mg kg^{-1}, respectively, at 60 cm. For Sb and Pb, an accumulation of PTE was measured at a depth of 10, and 60 cm.

3.2.2.4. Sediment cores from the mouth of the El Carrizal arroyo. In sediment core 1 (C1), the maximum As, Cd, Pb, Sb, and Zn concentrations were 186, 6.3, 58.9, 617, 55.5, and 377 mg kg^{-1}, respectively (Fig. 6). In sediment core 2 (C2), the As, Cd, Pb, Sb, and Zn concentrations were 112, 4.7, 54.6, 362, 19.6, and 281 mg kg^{-1},

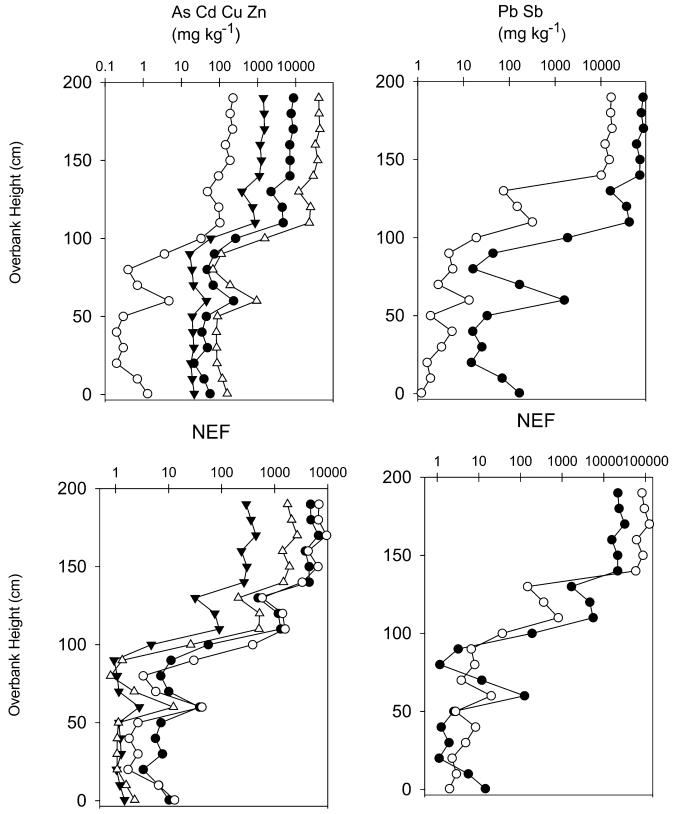

Fig. 4. The vertical profiles of As, Cd, Cu, Pb, Sb, and Zn concentrations and the Normalized Enrichment Factor distributions for the overbank. The graphs on the left are for As (filled circles), Cd (empty circles), Zn (empty triangles) and Cu (filled inverted triangles). The graphs of the right are for Sb (empty circles) and Pb (filled circles).

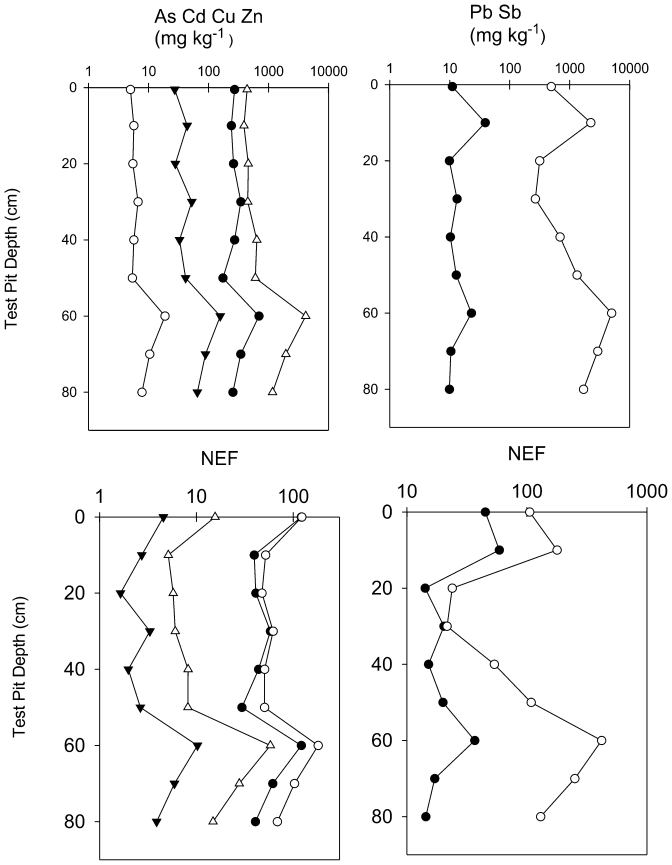

Fig. 5. Vertical profiles of the As, Cd, Cu, Pb, Sb, and Zn concentrations and the Normalized Enrichment Factor distributions in the test pit. The graphs of the left are for As (filled circles), Cd (empty circles), Zn (empty triangles) and Cu (filled inverted triangles) and the graphs of the right are for Sb (empty circles) and Pb (filled circles).

respectively (Fig. 7), which were greater than the average concentrations in the Earth's crust (Table 2). The As and Pb concentrations in C1 and C2 exceed those allowed by Mexican legislation (Table 2). These concentrations decreased in C2, and only As exceeded the value allowed by Mexican legislation.

The C1 and C2 vertical profiles are shorter than those for the OB and TP. The trace metal profiles in C1 were more homogeneous than those in the source (OB and TP). These concentrations increased to a maximum at depths of between 18 and 24 cm. The maximum As, Cd, Cu, Pb, Sb, and Zn concentrations were 186, 6.3, 53.8, 617, and 377 mg kg^{-1}, respectively (Fig. 6). The As, Cd, Cu, Pb, and Zn concentrations decreased with depth in C2 from a maximum at first 12 cm to a minimum at between 18 and 22 cm (Fig. 7).

4. Discussion

4.1. Normalized enrichment factors (NEFs)

The NEFs for the elements were calculated by using Al as a normalizing element (Rubio et al., 2000; Marmolejo-Rodríguez et al., 2007; Zourarah et al., 2007; Rashed, 2010). In regional sediments that are unaltered by anthropogenic activities, the mean Al concentrations (as a ratio of Fe or Li; Table 2) are similar to those determined by Wedepohl (1995). The background value concentration, used to calculate the NEFs was obtained from La

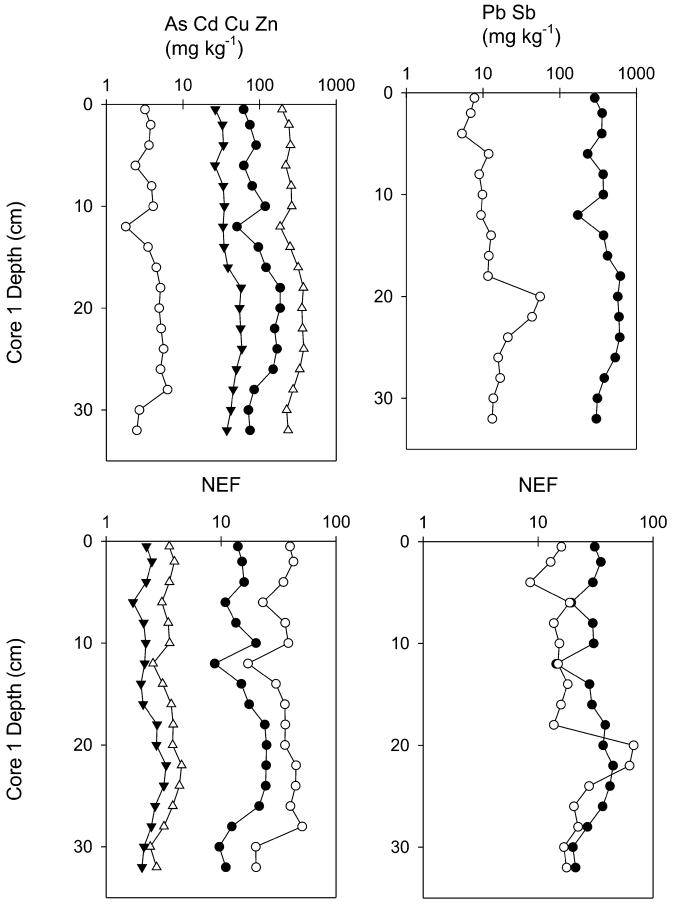

Fig. 6. Vertical profiles of the As, Cd, Cu, Pb, Sb, and Zn concentrations and the Normalized Enrichment Factor distribution in Core 1. The graphs of the left are for As (filled circles), Cd (empty circles), Zn (empty triangles) and Cu (filled inverted triangles) and the graphs of the right are for Sb (empty circles) and Pb (filled circles).

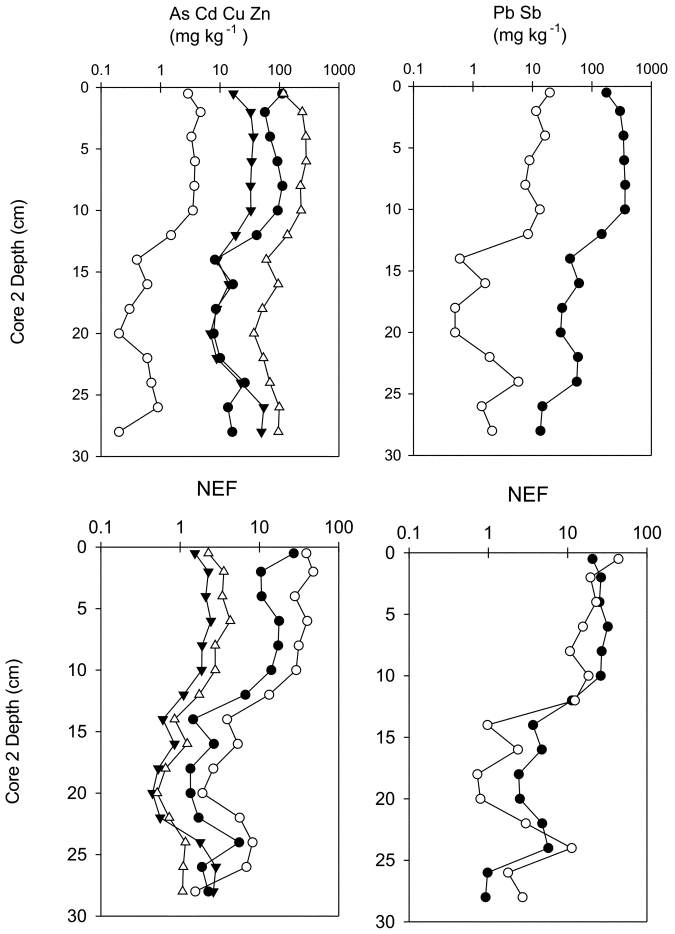

Fig. 7. Vertical profiles of the As, Cd, Cu, Pb, Sb, and Zn concentrations and the Normalized Enrichment Factor distributions in Core 2. The graphs on the left are for As (filled circles), Cd (empty circles), Zn (empty triangles) and Cu (filled inverted triangles) and the graphs of the right are for Sb (empty circles) and Pb (filled circles).

Noria (the pristine zone located in the same hydrological basin) (Fig. 1; Table 2) and was determined with the following equation:

$$\mathrm{NEF} = (\mathrm{Ei/Al})_{\mathrm{sed}}(\mathrm{Ei/Al})_{\mathrm{La\ Noria}} \quad (1)$$

Where $(\mathrm{Ei/Al})_{\mathrm{sed}}$ is the ratio between the element and aluminum concentrations in each sample, and $(\mathrm{Ei/Al})_{\mathrm{La\ Noria}}$ is the ratio between the element and aluminum concentrations in La Noria. The NEFs have no units because the values are divided by values with the same units.

The representative values for the enrichment levels are determined by normalizing values to a lithogenic element in systems that are impacted by anthropogenic activities (Audry et al., 2004; Borrego et al., 2004; Roychoudhury and Starke, 2006; Marmolejo-Rodríguez et al., 2007; Zourarah et al., 2007; Meza-Figueroa et al., 2009; Marmolejo-Rodríguez et al., 2011). For this NEF interpretation, we used a relative value scale that was adapted from Hakanson (1980), Cobelo-García and Prego (2004), and Marmolejo-Rodríguez et al., 2011.

NEF < 3 zero or null enrichment
NEF = 3–10 moderate enrichment
NEF = 10–25 severe enrichment
NEF = 25–50 very severe enrichment
NEF > 50 extremely severe enrichment

4.1.1. NEF vertical distribution and associations

The NEF vertical profiles for As, Cd, Pb, and Sb in the OB, TP, C1, and C2 (Figs. 4–7) clearly indicated anthropogenic incorporation of tailings into the OB. The NEF in the TP increased with depth (Fig. 5). The NEF in C1 and C2 (Figs. 6 and 7) although the NEF in C2 decreased from 10 to 20 cm and slightly increased from 20 to 30 cm, these variations were less pronounced than in C1.

4.1.1.1. NEF vertical distribution and associations in the overbank. The As, Cd, Cu, Pb, Sb, and Zn NEF intervals of between 110 and 200 cm were 56–6678, 382–9464, 90–442, 189–31,884, 807–124,246, and 504–2654, respectively. These results indicate an extremely severe enrichment (NEF > 50). The 110–200 cm range consists of fine red materials that correspond to tailings (layers B – E; Fig. 2a). This result indicates that mining wastes are the main contamination source for the H – G – C arroyo. However, the NEFs in the OB (Fig. 4) are similar to the mining wastes of Adak, Sweden (Ag, Pb, and Zn Mine; Bhattacharya et al., 2006) and are less enriched than the gold mining wastes of South Africa (Roychoudhury and Starke, 2006) and the arctic sediments from the Black Angel mine (Greenland; Perner et al., 2010).

4.1.1.2. NEF vertical distribution and associations in the test pit. The vertical distribution of the NEF is similar for all of the elements. The concentration decreases to a depth of 20 cm (Sand layer D, Fig. 2b) and increases with further depth. The NEFs are significantly less concentrated in the TP than in the OB. The TP has As, Cd, Cu, Pb, Sb, and Zn NEFs of 28–121, 47–180, 1.6–10, 23–420, 14–59, and 5.7–58, respectively (Fig. 5). These concentrations are extremely severe for As, Cd, Pb, Sb, and Zn and only moderate contamination for Cu (Fig. 5).

The concentrations of these elements can be diluted in the surface as they are transported along the arroyo basin from the source to the destination (Marmolejo-Rodríguez et al., 2011). However, these elements can become more concentrated with depth. The increased PTE concentrations in the TP occur because layer A resulted from a high energy event (Fig. 2b). This high energy event was potentially caused by a large landslide from the adjacent tailing pile. Thus, this layer contains mining wastes in a sand matrix. However, lower NEF values of 14–50 for As, Cd, Pb, and Sb occurred in layer C (20-cm depth; Figs. 2b and 5), which indicated severe enrichment and reflected a continuous deposit of fine and contaminated sediments (tailings) by low energy wind and rain.

4.1.1.3. NEF vertical distribution in sediment core 1 and 2. In sediment core 1, the NEF values for As, Cd, Cu, Pb, Sb, and Zn were 8.8–24.8, 17.2–50, 1.7–3.3, 14.3–44.8, 8.5–67, and 2.4–4.5 mg kg^{-1}, respectively. These values are significantly lower than those found in the OB and TP vertical distribution. In addition, these concentrations are larger than the previously determined concentrations in the surface sediments near the mouth of the arroyo (Marmolejo-Rodríguez et al., 2011). These results suggest that evaporitic basins favor the deposition of fine sediments, which are transported in the main arroyoflow or by wind. This evaporitic basin had several variables, including pH (8–8.9) and salinity (130–140‰), which favored flocculation, adsorption, and precipitation (Chester, 2003). The As and Cd NEF (Fig. 6) tended to decrease vertically in fine sands and accumulate in mud. This result confirmed that the elemental concentrations increase with decreasing grain-size mainly due to increased surface area, which increases adsorption (Salomons and Förstner, 1984; Kim et al., 2011). The C_{org} concentration increased relative to the concentrations in the OB and TP. The increased amounts of mud and C_{org} could be caused by the feedback of sediments from the arroyo bank from wind transport and changing water levels in the small lagoon. The sand in C1 potentially resulted from the introduction of materials during hurricanes in 2009.

C2 contained zero to severe As, Cd, Pb, and Sb contamination (NEF = 1.3–27, 1.5–48, 0.9–32, 0.72–43) and from null to moderate for Cu and Zn contamination (NEF = 0.44–2.8, 0.5–4.2). As, Cd, Pb, and Sb were more enriched in C1 than in C2 however, the Cu and Zn NEFs were similar between both cores. This decrease potentially occurred because C2 is farther from the El Carrizal arroyo discharge. Their vertical NEF distribution was similar for all elements (Fig. 7). The NEF values were highest in the first 12 cm and were lowest between 12 and 28 cm.

4.2. Multivariate analyses of the microenvironments

The climate, flora, and fauna are different at the source (496 masl) than at the mouth of the arroyo. To characterize the microenvironments in this system, multivariate analysis was used because different groups are formed for each matrix.

4.2.1. Overbank at the Hondo arroyo

The elements in the OB were highly correlated according to Principal Component Analysis (PCA; Fig. 8). The PTE (and their loads) of Zn (0.894), As (0.890), Cu (0.888), Pb (0.886), Cd (0.885), Fe (0.85), silt and clay (0.84), Sb (0.81), and C_{org} (0.74) were well-grouped (marked loadings > 0.74)) and were inversely correlated with Al (−0.84). This correlation represented Factor 1 and had a variance of 78%. In this matrix, the Fe concentrations were highly correlated with the silt and clay contents and the PTE were enriched. Although C_{org} was not enriched (<1%), it was highly correlated with the PTE concentrations. PTE were associated with silt and clay and most likely resulted from the tailing materials (Bhattacharya et al., 2006; Navarro-Flores and Doménech-Rubio, 2010). Factor 2 (9% of the variance) is represented by the grain-sizes of sand (0.92) and gravel (−0.85). These factors and Al are not associated with the As in the OB mine tailings. Geochemical processes, such as oxidation, can be observed in the OB and are evidenced by the large Fe concentrations (maximum contents 18%) that are associated with the PTE. In addition, Sb is enriched and associated with the PTE.

4.2.2. Test pit in the Hondo arroyo

The PCA of the TP (Fig. 8) were grouped into Factor 1 (Variance 53%) and dominated the PTE. The associated elements (with their respective loads) include Zn (0.974), Cd (0.967), Cu (0.939), As (0.936), and Pb (0.88). Factor 1 reflects anthropogenic enrichment. It was remarkable that these elements were associated in the absence of Sb although the TP was near (approximately 4 m) the OB. The Sb concentrations decreased relative to the OB tailings, which were reflected in the PCA. Factor 2 (Variance 18%) is represented by the lithogenic Al (0.91). Gravel (0.83), Fe (0.74), and Li (0.6) were included in Factor 2 but had less influence. Factor 2 was inversely related to sand (−0.82). In addition, Factor 1 was dominated by Zn (maximum contents of 4170 mg kg^{-1}). Corg concentrations were <0.3%. Therefore, geochemical, rather than organic, processes caused the downward migration of the elements. Although oxidation potentially occurred, the Fe concentrations (3–6.32%) were significantly lower than those in the OB at a distance of 4 m (Fe concentrations are presented in Table 2).

4.2.3. Sediment cores 1 and 2 in the El Carrizal arroyo

The evaporitic basin, where the main arroyo (H–G–C) discharge is near the Pacific Ocean, is influence by sandy sediments. However, although the sea was close by, this area had fine sediments (fine sand, silt, and clay).

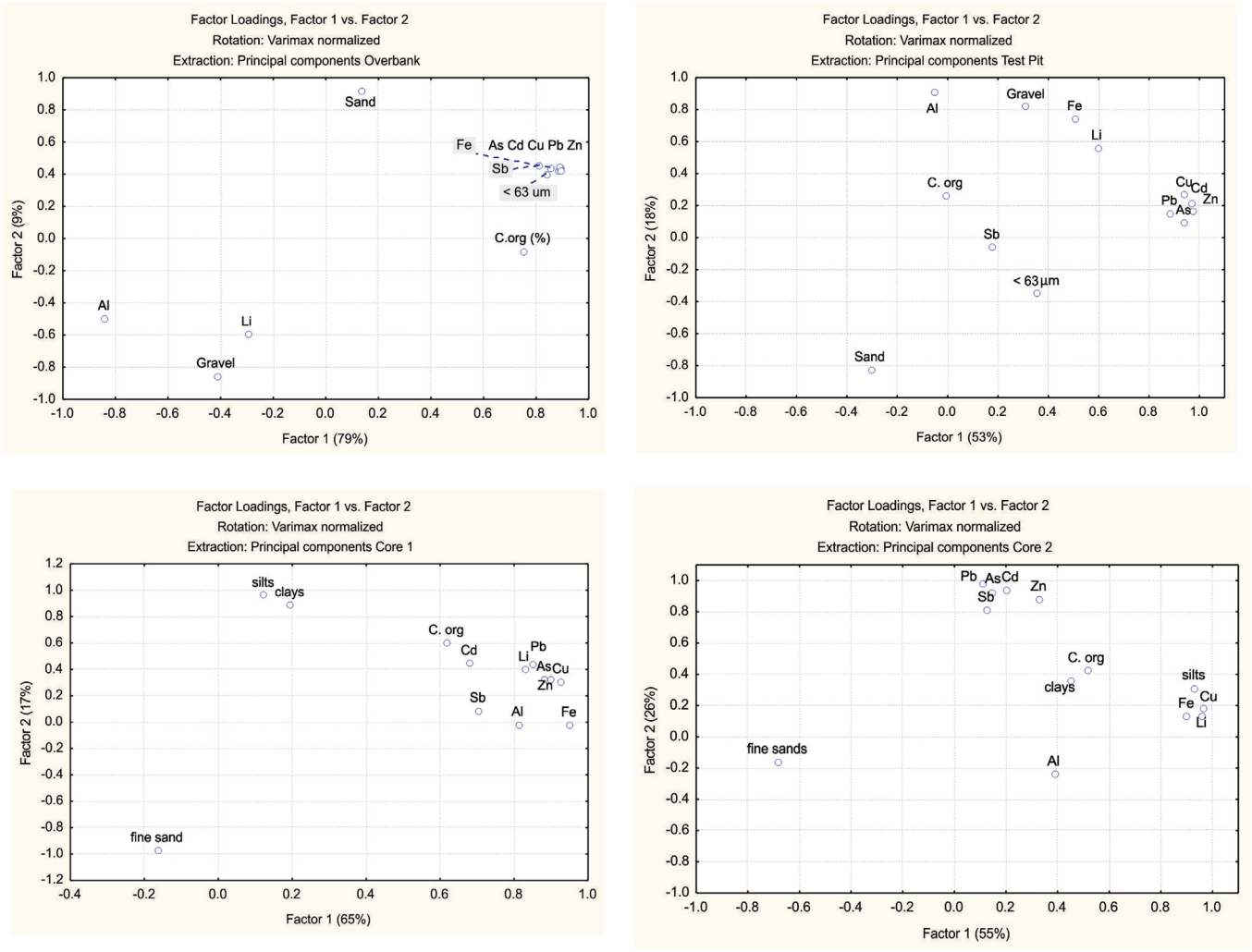

Fig. 8. Principal component analyses for the results from near the mining zone, the overbank, the test pit, and cores 1 and 2 at the discharge at the mouth of the arroyo.

The sediment cores behaved differently. Factor 1 in the C1 PCA (Fig. 8) was correlated with (with their loads) Fe (0.94), Cu (0.93), Zn (0.89), As (0.87), Pb (0.85), Li (0.83), Sb (0.70), and Al (0.81) (Variance = 65%). Factor 2 (Variance 17%) included grain size, silt (0.97), and clay (0.89) and was inversely correlated to fine sand (−0.97). Here, the anthropogenic influence of the PTE was disguised by the lithogenic elements, which resulted from the decreased PTE concentrations relative to the concentrations near the mining zone. This phenomenon is easily observed from the C2 PCA (Fig. 8), where Factor 1 (variance of 55%) is represented by the concentrations that are not enriched with Cu, Fe, Li, and silt, and Factor 2 (Variance 26%) is represented by the Pb (0.98), Cd (0.92), As (0.89), Sb (0.76), and Zn (0.88) PTE. The concentrations in C2 were less than half those in C1.

In both cores, the Corg concentration was greater than in the OB and TP (Figs. 2 and 3). Thus, biogeochemical processes became more important in the cores. In C1, the C_{org} (Fig. 3) was associated with Al and Fe PTE, which potentially resulted from its closer proximity to the arroyo mouth (10 m) than C2 (70 m). This distance could cause the concentration dilutions and the associations of Factor 1 with the terrigenous elements in C2. However, additional research is necessary to evaluate these processes in this hypersaline evaporitic basin.

4.2.4. Sample sites and their PTE concentration

The OB releases tailings into the arroyo. The influence of these tailings is observed from the TP, PTE concentrations because they are the closest sampling sites (Fig. 1). However, although the PTE concentrations reach contamination levels in the TP, their concentrations are relatively low and the resulting PCA distribution is different (Fig. 8). The PTE concentrations in the TP are diluted, most likely from the rainy season, extreme events, and wind, which scattered the PTE from the mine tailings of the OB throughout the arroyo.

In the evaporitic basin, the PTE only occur when the rain is intense. Greater concentrations occur in C1 because it is located directly in the discharge. The C2 is less influenced by discharge and has lower PTE concentrations than those in C1. However, in this study, the vertical accumulation of PTE in both cores corresponds with the sediments dilution that was observed by Marmolejo-Rodríguez et al. (2011).

4.3. Comparison between the El Triunfo – Pacific Ocean system and the tailings and sediments from other systems that were influenced by abandoned mines

The As, Cd, Cu, Pb, Sb, and Zn concentrations in the OB profile are comparable to those in other systems that are impacted by mining.

However, other studies did not determine the concentrations of all of these elements. Thus, we discuss each element separately below.

4.3.1. PTE in tailings

4.3.1.1. Arsenic. The amount of As in the OB mine tailings is comparable to the amount in mine tailings from other previously mined sites (Table 3). The maximum As concentration in the OB was similar to that observed in Au and Ag mine wastes in Massif, France (Bodénan et al., 2004), Zloty Stok, Poland (Krysiak and Karczewska, 2007), and Songsheon, South Korea (Lim et al., 2008). Specifically, in the La Soterraña, Spain Hg mine (Loredo et al., 2006), the maximum As concentrations were found in the presence of pyrite and arsenopyrite. Thus, serious contamination of the adjacent soils and aquifers occurred. Similar As migration processes are occurring in the aquifers that surround El Triunfo, which contains As concentrations of 400 mg L^{-1} (Carrillo, 1996).

4.3.1.2. Cadmium. The mean and maximum Cd concentrations in the OB are comparable to those in the Rio Marmato sediments (Colombia), which are affected by a gold mine (Prieto, 1998). In addition, these values are comparable to those found in the tailings and fluvial sediments that were affected by mining, extraction, and smelting activities of Pb and Zn minerals (Rudnaya River, Russia, Shulkin, 1997; Lot River, France, Audry et al., 2004; Black Angel Mine, Greenland, Perner et al., 2010). The Cd concentrations in these systems are associated with Zn minerals. Thus, Cd is found in the form of CdS in the sphalerite (Dana, 1944). The El Triunfo mine is rich in Zn (Marmolejo-Rodríguez et al., 2011) and Cd. Thus, Cd and Zn are associated in this system.

4.3.1.3. Copper, lead, and zinc. The mean and maximum Cu concentrations in the OB were comparable to those in Ag and Au mine tailings (Songsheon, South Korea, Lim et al., 2008; Sardinia, Italia, Da Pelo et al., 2009) and in Cu, Pb, and Zn mine tailings (Sambo, South Korea, Jung and Thornton, 1996; Mount Isa, Australia, Taylor and Hudson-Edwards, 2008; Santa Lucia, Cuba, Romero et al., 2010). These Pb and Zn concentrations contaminated the fluvial sediments (Pulford et al., 2009; Romero et al., 2010) and soils during rice cultivation (Jung and Thornton, 1996; Lim et al., 2008). Taylor and Hudson-Edwards (2008) determined that the overbanks near the mine zone had greater Cu concentrations and that Pb and Zn concentrations were significantly more concentrated in layers with a grain size of <2 mm in El Triunfo. Furthermore, these authors determined these concentrations in two different sized fractions (grain size <2 mm and <180 μm). However, the fine fraction was minimal in our study (Fig. 2). The concentrations of these elements were higher in our study because the tailings and/or mine wastes (ash) were mitigated along the fluvial basin.

4.3.1.4. Antimony. The mean and maximum Sb concentrations are greater than those found in the systems that were affected by Ag and Au mining (Marmato River, Colombia; Prieto, 1998; Ratotok Bay Indonesia, Edinger et al., 2007; Almería, Spain, Navarro-Flores and Doménech-Rubio, 2010). The Sb concentrations in the submarine tailings in Ratotok (490–580 mg kg^{-1}; Edinger et al., 2007) are comparable with the Sb concentrations in layer C (Figs. 2a and 4) of the OB.

The maximum PTE concentrations in the OB tended to decrease toward the base of the alluvial terrace. This phenomenon differs from that observed in the Australian overbanks (Taylor and Hudson-Edwards, 2008), where no clear tendency was shown. Here, the deposition is associated with recent mining. This tendency is similar to those observed in recently contaminated areas, such as the Tinto River (Spain; Borrego et al., 2004), Ruttjejaure Lake (Sweden; Bhattacharya et al., 2006), Pirhuacocha Lagoon (Peru; Cooke et al., 2007), Tindrum (Scotland, Pulford et al., 2009), and the Black Angel mine (Greenland, Perner et al., 2010).

4.3.2. The test pit, sediment cores 1 and 2

In the TP, the maximum and mean concentrations of As were similar to those in the other fluvial systems that were influenced by the Ag and Au mines (Sardinia, Italy, Da Pelo et al., 2009; Playazo Arroyo, Almería, España; Navarro-Flores and Doménech-Rubio, 2010). The As concentrations in C1 and C2 were similar to those found in sediments from the Tinto River, Spain, which were influenced by sulfur ores (Borrego et al., 2004). The Cd concentrations in

Table 3
Concentrations of As, Cd, Cu, Pb, Sb, and Zn in other systems in the world influenced by mining activities, they were compared in the text. Results in some cases were reported as: mean and *s*, or range, or maximum contents.

Systems influenced by mining activities, in the world	As (mg kg^{-1})	Cd (mg kg^{-1})	Cu (mg kg^{-1})	Pb (mg kg^{-1})	Sb (mg kg^{-1})	Zn (mg kg^{-1})	Reference
Tailings from Au–Ag mines South Korea							
Imcheon mine in Choongchung South Korea	n.d	0.6–9.4	27.0–229	142–8500	n.d.	283–1640	Jung, 2001
Songsheon mine, South Korea	3584–143,813	2.2–20	30–749	125–50,803	n.d.	580–7541	Lim et al., 2008
Au mine Chéni,Massif France.	6054 ± 0.26	n.d	n.d.	393 ± 1.26	n.d.	134 ± 1.22	Bodénan et al., 2004.
Zloty Stok and Zelezniak, Southwest of Poland	8690–15,800	n.d.	n.d.	n.d.	n.d.	n.d.	Krysiak and Karczewska, 2007
Furtei Sardinia, mine Italy	210–381	<0.5	196–690	130–73	n.d.	48–36	Da Pelo et al., 2009
Mine in Ratototok Bay North district of Silawesi, Indonesia	409–695	n.d.	n.d.	n.d.	490–580	n.d.	Edinger et al., 2007
Mine Almeria, Spain	71.5–1410	0.3–4.6	70.0–957	55.1–8744	4.2–253.0	91.0–1870	Navarro-Flores and Doménech-Rubio, 2010
Tailings in Pb–Zn mines							
Santa Lucia, mining zone, Cuba	1724	n.d.	811	22,700	n.d.	8300	Romero et al., 2010
Río Leichhardt, Mount Isa, Queensland Australia	n.d.	n.d.	370 ± 838	2000 ± 2210	n.d.	1600 ± 1000	Taylor and Hudson-Edwards, 2008
Fluvial sediments influenced by mining activities							
Rudnaya River, Russia	n.d.	47.2 ± 12.1	364 ± 86	1061 ± 151	n.d.	4227 ± 871	Shulkin, 1997
Marmato, Colombia Mining district	218–1850	28–240	129–619	330–22,800	6.8–56	1365–11,800	Prieto, 1998
Muñon Cimero mining area Asturias, Spain	26.8–28,060	n.d.	15.3–68.2	16.2–222	1.0–208	n.d.	Loredo et al., 2006
Tyndrum, Scotland, UK	n.d.	n.d.	n.d.	100–11,000	200–30,000	n.d.	Pulford et al., 2009
Sedimentary cores							
Lot River, France	n.d.	127	97.72	523	n.d.	4430	Audry et al., 2004
Black Ángel mine Maarmorilik Greenland.	Max 61.1	Max 74.1	n.d.	Max 7800	n.d.	Max 15,400	Perner et al., 2010.

the TP were similar to those of Ag, Au, Pb and Zn in soils and tailings from South Korea (Jung and Thornton, 1996; Lim et al., 2008). The Cd concentrations in C1 and C2 were similar to those in tailings from Incheon, Korea (Jung, 2001) and Almeria, Spain (Navarro-Flores and Doménech-Rubio, 2010). The copper concentrations in the C1 and C2 TP samples were similar to those in the arroyo sediments near mining sites with low Cu concentrations (La Soterraña, Asturias, Spain, Loredo et al., 2006). The antimony concentrations in the C1 and C2 TP samples were similar to those in sediments from the Marmato River (Colombia, Prieto, 1998). The Pb and Zn concentrations in the TP were similar to those in the fluvial sediments that were influenced by Au and Ag mines (Pirhuacucha Lagoon, Peru, Cooke et al., 2007; Playazo Arroyo, Almería Spain, Navarro-Flores and Doménech-Rubio, 2010) and in fluvial systems that were near Pb and Zn mines (Rudnaya River Russia, Shulkin, 1997; Mount Isa River, Australia, Taylor and Hudson-Edwards, 2008; Sta. Lucía, Cuba, Romero et al., 2010). The Pb and Zn in the C1 and C2 are similar to tailings in Massif, France (Bodénan et al., 2004). Our results (along with those of Kossoff et al. (2012)) strongly suggest that the release of tailings into floodplains should be limited or prohibited. In addition, our results suggest that all tailings should be removed from floodplains following dam overflow, such as those at the OB.

5. Conclusions

The abandoned gold mine at El Triunfo is an important source of potential toxic elements, such as As, Cd, Pb, Sb, and Zn. The overbank sites, which contain large quantities of the tailings, are the most contaminated sites with extremely severe anthropogenic enrichment of PTE. The arroyo sediments in the TP are severely enriched with As, Pb, Sb, and Zn. This contamination is exacerbated by extreme weather events, which were observed from the sedimentary sequence. The sediment cores that were approximately 49-km from the source (mining district, overbank, and test pit) were severely enriched with As, Cd, Pb, and Sb. The C1 core was more contaminated because it was directly affected by the arroyo discharge. The contamination was diluted 500-m from the discharge (C2). In the discharge, the maximum concentrations were correlated with C_{org} concentrations and silt contents.

Acknowledgments

This research was made possible by the support of the Projects SIP 20120697, 20110874 from the Instituto Politécnico Nacional (Mexico). In addition, the authors thank Dr. Ellis Glazier for editing the English text.

References

Acosta, B., Méndez, L., Ortega, A., 2000. Recomendaciones ambientales para la restauración del Complejo minero “El Triunfo” B.C.S. CIBNOR. Technical Report. (in Spanish).

Audry, S., Schäfer, J., Blanc, G., Jouameau, J.M., 2004. Fifty-year sedimentary record of heavy metal pollution (Cd, Zn, Cu, Pb) in the Lot River reservoirs (France). Environmental Pollution 132, 41–426.

Bhattacharya, A., Routh, J., Jacks, G., Bhattacharya, P., Mörth, Magnus, 2006. Environmental assessment of abandoned mine tailings in Adak Västerbotten, district (northern Swedens). Applied Geochemisty 21, 1760–1780.

Bodénan, F., Baranger, P., Piantone, P., Lassin, A., Azaroual, M., Gaucher, E., Braibant, G., 2004. Arsenic behaviour in gold-ore mill tailings, Massif Central, France: hydrogeochemical study and investigation of in situ redox signatures. Applied Geochemistry 19, 1785–1800.

Borrego, J., López-González, N., Carro, B., 2004. Geochemical signature, as paleoenvironmental markers in Holocene sediments of the Tinto River estuary (Southwestern Spain). Estuarine. Coastal and Shelf Science 61, 631–641.

Carrillo, A., 1996. Environmental Geochemistry of the San Antonio-El Triunfo Mining Area. Wyomig United States of America, Southernmost Baja California Peninsula, México. Laramie, p. 130. Ph.D, Thesis in Geology.

Chester, R., 2003. Marine Geochemistry, second ed. Blackwell Science Ltd.

Cobelo-García, A., Prego, R., 2004. Influence of point sources on trace metal contamination and distribution in a semi-enclosed industrial embayment: the Ferrol Ria (NW Spain). Estuarine Coastal and Shelf Science 60, 695–703.

Cooke, C.A., Abbott, M.B., Wolfe, A.P., Kitleson, J.L., 2007. A millennium of metallurgy record by lake sediments from Morococha, Peruvian Andes. Environmental Sciences and Technology 41, 3469–3474.

COREMI, 1999. Monografía geológico-minera del estado de Baja California Sru. Secretaría de Comercio y Fomento Industrial. Coordinación General de Minería, México, p. 237 (in Spanish).

Dana, J.D.,E.S., 1944. In: . In: Palache, C., Berman, H., Frondel, C. (Eds.), System of Mineralogy, seventh ed., vol. 1. (New York).

Da Pelo, S., Musu, E., Cidu, R., Frau, F., Lattanzi, P., 2009. Release of toxic elements from rocks and mine wastes at the Furtei gold mine (Sardinia, Italy). Journal of Geochemical Exploration 100, 147–152.

Edinger, E.N., Siegar, P.R., Blackwood, G., 2007. Heavy metal concentration in shallow marine sediments affected by submarine tailing disposal and artisanal gold mining Buyat-Ratototok district North Sulawesi, Indonesia. Environmental Geology 52, 701–714.

Hakanson, L., 1980. An Ecological risk index for aquatic pollution control. A sedimentological approach. Water Research 14, 975–1001.

Jung, M.C., Thornton, I., 1996. Heavy metal contamination of soils and plants in the vecinity of a lead-zinc mine, Korea. Applied Geochemistry 11, 53–59.

Jung, M.C., 2001. Heavy metal contamination of soil and waters in and around the Imcheon Au-Ag mine Korea. Applied Geochemistry 16, 1369–1375.

Kim, C.S., Wilson, K.M., Rytuba, J., 2011. Particle-size dependence on metal(loid) distributions in marine wastes. Implication for water contamination and human exposure. Applied Geochemistry 26, 484–495.

Kossoff, D., Hudson-Edwards, K.A., Dubbin, W.E., Alfredsson, M., 2012. Major and trace metal mobility during weathering of mine tailings: Implications for flood plain soils. Applied Geochemistry 27, 562–576.

Kovács, E., Dubbin, W., Tomás, J., 2006. Influence of hydrology on heavy metal speciation and mobility in a Pb-Zn mine Tailing. Environmental Pollution 141, 310–320.

Krysiak, A., Karczewska, A., 2007. Arsenic extractability in soils in the areas of former arsenic mining and smelting, SW Poland. Science of the Total Environment 379, 190–200.

Lim, H.S., Lee, J.-S., Chon, H.-T., Sager, M., 2008. Heavy metal contamination and health risk assessment in the vicinity of the abandoned Songcheon Au-Ag mine in Korea. Journal of Geochemical Exploration 96, 223–230.

Loredo, J., Ordoñez, A., Álvarez, R., 2006. Environmental impact of toxic metal and metalloids from the Muñon Cimero mercury-mining area (Asturias, Spain). Journal of Hazardous Materials 136, 455–467.

Marmolejo-Rodríguez, J., Prego, R., Meyer-Willerer, A., Shumilin, E., Cobelo-García, A., 2007. Total and labile metals in surface sediments of the tropical river-estuary system of Marabasco (Pacific coast of México): influence of an iron mine. Marine Pollution Bulletin 55, 459–468.

Marmolejo-Rodríguez, A.J., Sánchez-Martínez, M.A., Romero-Guadarrama, J.A., Sánchez-González, A., Magallanes-Ordóñez, V.R., 2011. Migration of As, Hg, Pb, and Zn in arroyo sediments from a semiarid costal system influenced by the abandoned gold mining district at El Triunfo, Baja California Sur. México. Journal of Environmental Monitoring 13, 2182–2188.

Meza-Figueroa, D., Maier, R., De la O-Villanueva, M., Gómez-Alvarez, A., Moreno-Zazueta, A., Rivera, J., Campillo, A., Grandlic, C., Anaya, R., Palafox-Reyes, J., 2009. The impact of unconfined mine tailings in residencial areas from a mining town in a semi-arid environment: Nacosari, Sonora, México. Chemosphere 27, 140–147.

Naranjo, A., 2004. Estudio de la Contaminación por Arsénico en agua, suelo y plantas de la Región del Cabo en Baja California Sur, México. Master Thesis. UNAM (in Spanish).

Navarro-Flores, A., Doménech-Rubio, L., 2010. Arsenic and metal mobility from Au mine tailings in Rodalquilar (Almería SE Spain). Environment Earth Science 60, 121–138.

NOM-147-SEMARNAT/SSA1-2004. Que establece criterios para determinar las concentraciones de remediación de suelos contaminados por arsénico, bario, berilio, cadmio, cromo hexavalente, mercurio, níquel, plata, plomo, selenio, talio y vanadio. In spanish, Mexican Legislation, Official Report. (in Spanish).

Nriagu, J.O., Pacyna, J.M., 1988. Quantitative assesment of worldwide contamination of air, water and soils by trace metals. Nature 333, 134–139.

Perner, K., Leipe, Th., Dellwig, O., Kuijipers, A., Mikkelsen, N., Andersen, T.J., Harff, J., 2010. Contamination of arctic Fjord sediments by Pb-Zn mining at Maarmorilik in central west Greenland. Marine Pollution Bulletin 60, 1065–1073.

Price, G., Winkle, K., Gehrels, W.R., 2005. A geochemical record of the mining history of the Erme Estuary, South Devon, UK. Marine Pollution Bulletin 50, 1706–1712.

Prieto, G., 1998. Geochemistry of heavy metals derived from gold-bearing sulphide minerals in the Marmato district (Colombia). Journal of Geochemical Exploration 64, 215–222.

Pulford, L.D., Mackenzie, A.B., Donatello, S., Hastings, L., 2009. Source term characterisation using concentration trends and geochemical associations of Pb ans Zn in river sedinments in the vicinity of a disused mine site: Implications for contaminant metal dispersion process. Environmental Pollution 157, 1649–1656.

Rashed, M.N., 2010. Monitoring of contaminated toxic and heavy metals, from mine tailings through age accumulation, in soil and some wild plant at Southeast Egypt. Journal of Hazardous Materials 178, 739–746.

Romero, F., Prol-Ledesma, R.M., Núñes-Alvares, L., Pérez-Vázquez, R., 2010. Acid drainage at the inactive Santa Lucia mine, western Cuba: natural attenuation of arsenic, barium and lead, and geochemical behavior of rare earth elements. Applied Geochemistry 25, 716–727.

Romero-Guadarrama, J.A., 2011. Geoquímica de As, Hg, Pb y Zn y mineralogía en sedimentos superficiales de la Cuenca de drenaje del distrito minero El Triunfo, B.C.S., México. Master Thesis. Instituto Politécnico Nacional, Mexico (in Spanish).

Roychoudhury, A.N., Starke, M.F., 2006. Parttioning and mobility of trace metals in the Blesbokspruit: impact assessment of dewatering of mine waters in the East Rand, South Africa. Applied Geochemistry 21, 1044–1063.

Rubio, B., Nombella, M.A.., Villas, F., 2000. Geochemistry of major and trace elements in sediments of Ria de Vigo (NW Spain): an a assessment of metal pollution. Marine Pollution Bulletin 40, 968–980.

Salomons, W., Förstner, U., 1984. Metals in the Hydrocycle. Springer-Verlag, New York, p. 349.

Salomons, S.W., 1995. Environmental impact of metals derived from mining activities; processes, predictions, prevention. Journal of Geochemical. Exploration 52, 5–23.

Shulkin, V.M., 1997. Pollution of the coastal bottom sediments at the Middle Primorie (Russia) due to mining activity. Environmental Pollution 101, 401–404.

Taylor, M.P., Hudson-Edwards, K.A., 2008. The dispersal and storage of sediment-associated metals in an arid river system: the Leichhard River Mount Isa, Queensland, Australia. Environmental Pollution 152, 193–204.

Troyo-Diéguez, E., Lachica-Bonilla, F., Fernández-Zayas, J.L., 1990. A simple aridity equation for agricultural purposes in marginal zones. Journal In Dry Environmental 19, 353–362.

Volke-Sepúlveda, T., Solórzano, G., Rosas, A., Izumikawa, C., Aguilar, G., Velasco, J., Flores, S., 2003. Remediación de sitios contaminados por metales provenientes de jales mineros en los distritos de El Triunfo-San Antonio y Santa Rosalía, Baja California, Sur. CENICA. National Institute of Ecology, Mexico. Technical Report. (in Spanish).

Wedepohl, K.H., 1995. The continental crust. Geochimica et Cosmochimica Acta 59, 1217–1232.

Zourarah, B., Maanan, M., Carruesco, C., Aajjane, A., Mehdi, K., Freitas, M.C., 2007. Fifty-year sedimentary record of heavy metal pollution in the lagoon of Oualidia (Moroccan Atlantic coast). Estuarine Coastal and Shelf Science 72, 359–369.